Supplementary Information

Vehicle emissions of short-lived and long-lived climate forcers: trends and tradeoffs

Morgan R. Edwards[a‡], Magdalena M. Klemun[a‡], Hyung Chul Kim[b], Timothy J. Wallington[b], Sandra L. Winkler[b], Michael A. Tamor[b], Jessika E. Trancik[a]

[a] *Massachusetts Institute of Technology, Cambridge, Massachusetts 02139, USA*. E-mail: trancik@mit.edu
[b] *Research & Advanced Engineering, Ford Motor Company, Dearborn, Michigan 48121-2053, USA.* Email: twalling@ford.com
‡ Contributed equally.

Table S1: Introduction year for diesel HDV emission standards used in the model

Region	Uncontrolled	Engine Models	Euro 1	Euro 2	Euro 3	Euro 4	Euro 5	Euro 6
U.S.	1960	1990	1992	1996	2001		2004	2007
Canada	1960	1990	1992	1996	2001		2004	2007
Mexico	1960	1990	1995	1998	2003	2008		
Brazil	1960	1993	1996	2000	2006		2012	
Latin America-31	1960		2000	2010	2015	2020		
EU-27	1960		1992	1997	2001	2006	2009	2013
Russia	1960		1999	2006	2008	2010	2014	
Non-EU Europe	1960		2000	2010	2015	2020		
China	1960		2001	2004	2008	2013	2017	2020
Japan	1960	1988	1994	1997	2003	2005		2009
India	1960	1992	2000	2003	2005	2010		2020
South Korea	1960	1990	1995	1998	2008	2010		2014
Australia	1960	1976	1995		2003	2008	2011	
Asia-Pacific-40	1960		2005	2010	2015	2020		
Middle East	1960		2000	2015	2020	2025		
Africa	1960	2000	2005	2015	2020	2025		

S1. Computation of LDV emission factors

In computing the light-duty vehicle (LDV) emission factors in Tables 1 and 2, we equate emissions for vehicles certified to Euro 1, 2, 3, 4, 5, and 6 standards to those for 1990, 1990-1994, 1995-2003, 2004-2007, 2006-2009, and 2008-2020 model years in the U.S., respectively, using MOVES data from Tables A2-A5 in Cai et al. (2013). The Euro-equivalent years are based on the ICCT Roadmap Model's values (ICCT 2012) for the emission standards introduction year in the U.S. (Table 3). Similarly for diesel heavy-duty vehicle (HDV) emission factors (Table 4), we use the ICCT Model equivalence years (Table

S1) to equate the Euro I-VI vehicle emissions to the 1992-1995, 1996-2000, 2001-2003, 2002-2005, 2004-2006, and 2007-2020, respectively, U.S. MOVES emission factors (Table A22, Cai et al. 2013). We retain our MOVES-calculated Euro 5 HDV diesel emission factors for Euro 6 because the original MOVES emission factors in Cai et al (2013) increase by a factor of 100 from 2006 to 2007 without explanation. We retain the ICCT default values for uncontrolled LDVs and HDVs and vehicles with engine modifications (but no emission control system) in Tables 1, 2 and 4, with a few exceptions. The NO_x and CO data for uncontrolled and engine modified gasoline LDVs in Table S1 are those reported for 1957-1962 and 1969-1971 model year vehicles (Fegraus et al. 1973, Wallington et al. 2008). The HDV engine modification factors in Table 4 are from 1990 MOVES data (Table A22, Cai et al. 2013).

In contrast to gasoline vehicles, less progress was achieved in reducing NO_x emissions from diesel LDVs. This can be seen by comparing the Euro 5 and Euro 6 data in Tables 1 and 2. It has been widely recognized that the decrease in NO_x emissions from diesel vehicles in the real world has been less than expected based on emission standards as tested under laboratory conditions (Carslaw et al. 2011, Carslaw and Rhys-Tyler 2013, Weiss et al. 2011, Chen and Borken-Kleefeld 2014, Velders et al. 2011). As a consequence, real driving emission (RDE) limits in Europe have been implemented in two steps with step 1 in September 2017 and step 2 in January 2020. These RDE steps are expected to lead to a substantial reduction in NO_x emissions from diesel LDVs. In the present work, we assume a NO_x emission factor of 0.15 g $(km)^{-1}$ for 2020 model year diesel LDVs based on the scenarios considered in Figure 4 of Toenges-Schuller et al. (2016).

S2. Engine emission profiles

The vast majority of road vehicles are powered by four-stroke internal combustion engines using either gasoline or diesel fuel. Diesel and gasoline engines have fundamentally different modes of operation. In gasoline engines the homogeneous air-fuel mixture is ignited by a spark. The flame travels smoothly across the combustion chamber, heating the gases and driving down the piston. In diesel engines, the fuel autoignites as it is sprayed at high pressure into compressed hot air in the combustion chamber. A spark is not required to ignite the diesel fuel, which is a heavier, less volatile mixture of hydrocarbons than gasoline and chemically more susceptible to autoignition.

Relative to gasoline engines, diesel engines have higher compression ratios, more rapid combustion, lower throttling losses, and operate leaner (i.e., at a greater air-fuel ratio). As a result, diesel engines generally exhibit higher efficiency than gasoline engines. Diesel fuel also has approximately 12% greater volumetric energy content than gasoline, and diesel engines in conventional (i.e. non-hybrid) vehicles

generally operate with roughly 30-40% higher volumetric fuel economy (lower fuel consumption) than similar gasoline vehicles (Sullivan et al. 2004, Elgowainy et al. 2016). Diesel engines must be mechanically robust to higher pressures, have more complex fuel systems, and are more expensive to manufacture than gasoline engines. This disadvantage is offset by their relatively low fuel consumption and generally higher durability. In high-mileage and heavy-load commercial vehicle applications, the fuel cost savings typically outweigh the increased engine cost.

Exhaust from internal combustion engines contains CO_2, CO, hydrocarbons and volatile organic compounds (VOCs), nitrogen oxides (NO_x), nitrous oxide (N_2O), methane (CH_4), and particulate matter (PM). Hydrocarbon and VOC emissions are unburnt or partially burnt fuel. CO is partially burnt fuel. NOx is formed by the Zeldovich mechanism. This mechanism is initiated by thermal dissociation of oxygen molecules to give oxygen atoms, which react with molecular nitrogen to produce NO (Zeldovich 1946). Particulate matter emissions stem from oxygen-deficient combustion and from pyrolysis of fuel droplets. Black carbon, also known as soot, is a component of PM that is operationally defined based on measurement of light absorption and chemical reactivity and/or thermal stability (IPCC 2013). In contrast to gasoline vehicles which operate at, or close to, stoichiometry, diesel engines operate lean (i.e., with an excess of air to fuel) and at lower temperatures than gasoline engines. Hence the VOC, CO, and NOx emissions from diesel engines are generally lower than for gasoline engines. Diesel fuel is less volatile than gasoline, and pyrolysis of fuel droplets is generally more important in diesel engines. As a result, emissions of PM are generally higher for diesel engines than for gasoline engines.

Diesel exhaust consists mainly of N_2 and O_2 (typically approximately 8-10%, but it can be as high as 20% during idle or as low as 6% during filter regeneration), CO_2, and H_2O. Diesel oxidation catalysts, typically Pd and Pt, are used to treat CO and VOCs. While diesel engines typically produce less NO_x than gasoline engines, significant amounts of O_2 in diesel exhaust make the treatment of NO_x in the emissions control system more challenging. The technology used to treat NOx in diesel exhaust is either lean NO_x traps (LNTs) or selective catalytic reduction (SCR). In LNTs, the NO_x is trapped during lean operation and reduced in rich transients. In SCR systems, ammonia is used to selectively reduce NOx over a Cu/zeolite catalyst.

S3. Comparison of emissions and trends from Section 3.1 (main paper) with literature data

It is important to validate results from emission models by comparing them with experimental measurements. Field measurements using remote sensing techniques have been used to measure emissions

from the on road LDV fleet in Chicago. Non-dispersive IR spectroscopic monitoring techniques were used for CO, CO_2, and HC, and dispersive UV spectroscopic monitoring techniques were used for NO and NO_2, SO_2 and NH_3. Measurements were conducted in 1997, 1998, 1999, 2000, 2002, 2004, 2006, and 2014 with approximately 20,000 vehicles measured in each study and pollutants measured relative to CO_2 emissions (Bishop and Stedman 2015). Over the period 2000 to 2014, the mean emission factors measured for CO and NO_x relative to CO_2 decreased from 1.04×10^{-2} to 3.0×10^{-3} g (g CO_2)$^{-1}$ and 1.4×10^{-3} to 4.8×10^{-4} g (g CO_2)$^{-1}$, respectively. As shown in Figure S1, the rates of change in CO and NO_x emissions observed from LDVs in Chicago in 2000-2014 are similar to those estimated for the U.S. LDV fleet in the present work, but the absolute magnitude of the emissions are approximately a factor of 2 lower.

The emissions from the MOVES model capture all phases of vehicle operation, including critically cold starts. For modern vehicles, a large fraction of vehicle emissions occur during cold start, when the engine and catalyst are warming up to their optimal operating temperatures (Wallington et al. 2006, Weilenmann et al. 2014). It is therefore reasonable that emissions measured from vehicles already warmed up, including on the freeway on-ramp in Chicago and other measurement date sources considered below, will be lower than those from the MOVES model.

Vehicle emission measurements performed in 2013-2014 in Toronto, with plumes captured for 103,000 vehicles and traffic shares of 97% LDVs and 3% HDVs, were reported by Wang et al. (2015). Mean emission factors for NO_x, CO, and black carbon (BC) were 2.3 g (kg fuel)$^{-1}$, 10 g (kg fuel)$^{-1}$, and 35 mg (kg fuel)$^{-1}$, respectively. A carbon weight fraction of 0.86 was assumed for fuel. Normalized to CO_2, the emission factors for NO_x, CO, and BC were 7.3×10^{-4}, 3.2×10^{-3}, and 1.1×10^{-5} g (g CO_2)$^{-1}$, respectively. The vehicle fleet in Canada is similar to that in the U.S., and it is reasonable to compare the results from Wang et al (2015) with our estimates for the U.S. The NO_x and CO emissions measured in Toronto are lower by factors of approximately 2 and 3, and the BC emissions are higher by approximately 20%, compared to those we estimate for the LDV fleet in the U.S. The lower NO_x and CO emissions observed in the remote sensing measurements in Toronto probably reflect few, if any, cold starts and hence would be expected to be lower than those derived from the MOVES model. BC emissions are less affected by catalyst temperature and hence are close to those estimated from the MOVES data.

Zhou et al. (2007) used remote sensing to measure CO and NO_x emissions from gasoline LDVs in Beijing in 2004. Emissions of CO were approximately 17 and 10 g/km, and emissions of NO_x were approximately 1.25 and 0.5 g/km for vehicles meeting Euro 1 and Euro 2 standards, respectively. These results are consistent, within a factor of 2, with those used in the present study as given in Table S1. Vehicle emission studies conducted in urban traffic tunnels in China have shown a decrease of CO and

NO_x per vehicle per km emissions of approximately 90% over the past 20 years. In the most recent published study, emissions of CO and NO_x from the mixed traffic flow (more than 90% gasoline LDVs) in tunnels in Changsha and Shanghai in 2012 and 2013 (with grades ranging from -6% to +6%) were reported as 0.754-6.050 g (vehicle km)$^{-1}$ and 0.12-0.82 g (vehicle km)$^{-1}$, respectively (Deng et al. 2015). The midpoints of these ranges are approximately a factor of 2 lower than our estimates for the on-road fleet in 2010-2015. Again, the difference probably reflects the fact that vehicles in the tunnel have warm engines and catalyst systems.

Carslaw and Rhys-Tyler (2013) have reported estimates for NO_x emissions from Euro 1 to Euro 5 gasoline and diesel passenger cars based on remote sensing measurements of 33,000 vehicles in four locations in London. Carslaw and Rhys-Tyler (2013) measured NO_x emissions relative to CO_2 emissions and reported the volume ratio NO_x/CO_2. Taking emissions of 230 g CO_2/km and 190 g CO_2/km for gasoline and diesel LDVs from the ICCT model we can place the volume ratios from Carslaw and Rhys-Tyler (2013) on an absolute mass basis as shown in Table S2. The right hand two columns give the ratio of the values derived from the MOVES model used in the present work to those reported by Carslaw and Rhys-Tyler (2013). As seen from Table S2 the MOVES-derived data are generally larger than those measured by Carslaw and Rhys-Tyler (2013). The 95% confidence interval uncertainty in the measurements by Carslaw and Rhys-Tyler (2013) is typically approximately 10%. The generally higher MOVES data again probably reflects the fact that these are lifetime average vehicle emissions, which include cold starts, while the data from Carslaw and Rhys-Tyler (2013) are from vehicles which are warmed up and operating on major roads in London.

Table S2: NO_x emissions reported by Carslaw and Rhys-Tyler for Euro 1-5 gasoline and diesel LDVs compared to values derived from the EPA MOVES model used in the present work.

	Carslaw and Rhys-Tyler (2013) NO_x/CO_2 [a]		ICCT CO_2 [b]		Carslaw and Rhys-Tyler (2013) NO_x		MOVES NO_x [c]		MOVES/ Carslaw and Rhys-Tyler (2013) [d]	
	10000 (v/v)		g/km	g/km	g/km	g/km	g/km	g/km		
Euro	Gasoline	Diesel	Gasoline	Diesel	Gasoline	Diesel	Gasoline	Diesel	Gasoline	Diesel
1	54.1±6.5	55.7±7.4	230	190	1.30	1.11	2.07	2.53	1.6	2.29
2	39.3±2.4	65.5±4.1	230	190	0.94	1.30	2.07	2.33	2.2	1.79
3	15.3±1	62.9±1.5	230	190	0.37	1.25	0.94	2.01	2.6	1.61
4	10.3±0.7	47.7±0.9	230	190	0.25	0.95	0.29	1.72	1.2	1.82
5	4.8±0.7	49.9±1	230	190	0.12	0.99	0.19	0.89	1.7	0.90

a. Data from Table 2 in Carslaw and Rhys-Tyler (2013); b. Calculated from energy efficiencies of 3.15 MJ/km and 2.58 MJ/km for gasoline and diesel LDVs and 72.44 gCO_2/MJ for gasoline and 74.06 g CO_2/MJ for diesel in the ICCT Model; c. Used in this work; d. Ratio of lifecycle emission value used in this work to that derived from on-road measurements by Carslaw and Rhys-Tyler (2013).

Exceedances of ambient air quality NO_2 standards are a significant issue in many European cities. It is well established that the ratio of NO_2 to NO_x in exhaust from some diesel vehicles increased in the 2000s, reflecting the increased use of technology that used NO_2 to oxidize soot in DPFs in HDVs. The latest real world emission studies (Carslaw et al. 2016) indicate that primary NO_2 emissions peaked in approximately 2010 and have since been falling, reflecting improvements in the emission control technology. Among air quality monitoring sites in Germany that are influenced by road traffic, the fraction that exceed the air quality limit for annual mean NO_2 is expected to fall from 50% in 2015 to 1-4% in 2030 (Toenges-Schuller et al. 2016).

The International Energy Agency (IEA) developed the Sustainable Mobility Project (SMP) model in 2002 to 2004, which provides estimates of emissions of NO_x, CO, and CO_2 from the global LDV and HDV fleet over the period 2000- 2050 (WBCSD 2004). The SMP model provides estimates of global tank-to-wheel (TTW) emissions in 2000 and 2030 for: NO_x from LDVs, 9.0 and 1.6 Mt; NO_x from HDVs, 10.6 and 3.7 Mt; CO from LDVs, 197.6 and 20.1 Mt; and CO from HDVs, 5.5 and 1.1 Mt. The 2000 data in Figure S5 are consistent with those in the SMP model, but the rates of emission decreases estimated in the present work are less than those projected in the SMP model. These differences reflect an improved understanding of real-world emission performance.

The EDGAR database maintained by the European Commission (EC 2014) contains estimates of global emissions by sector for CO_2, CO, CH_4, NO_x, and N_2O for 2000-2008. Figure S3 shows the excellent agreement for global CO_2, CO, and NO_x emissions (both absolute magnitudes and trends) between EDGAR for the road transport sector and the sum of LDV and HDV emissions estimated in our analysis.

The EDGAR database has approximately a factor of 4 lower, and significantly smaller downward trend in, CH_4 emissions over the period 2000-2008 than our results. Our emission factor of 2.0×10^{-4} g CH_4 (g CO_2)$^{-1}$ for the US LDV fleet in 2000 shown in Figure S2 is slightly higher than the estimate of $(1.5 \pm 0.4) \times 10^{-4}$ g CH_4 (g CO_2)$^{-1}$ based on vehicle dynamometer data for 1995-1999 model year vehicles reported by Nam et al. (2004). We are not able to offer a rationalization of the discrepancy between our estimate of TTW CH_4 emissions and the approximately factor of 4 lower value in the EDGAR database. Further work is warranted to understand this discrepancy.

The EDGAR database has approximately a factor of 2 lower N_2O emissions over the period 2000-2008 than our results. The emission estimates for the global LDV and HDV fleets in 2010 of 112×10^{-6} g N_2O (g CO_2)$^{-1}$ and 20×10^{-6} g N_2O (g CO_2)$^{-1}$ from the present work shown in Figure S1 can be compared with the ranges of 31-57 $\times 10^{-6}$ g N_2O (g CO_2)$^{-1}$ and 7-56 $\times 10^{-6}$ g N_2O (g CO_2)$^{-1}$ respectively, by Wallington

and Wiesen (2014). Our estimate for the LDV fleet in Figure S1 is approximately a factor of 2 greater than the upper limit of the range estimated by Wallington and Wiesen (2014). Our estimate for the HDV fleet in Figure S1 lies close to the middle of the range estimated by Wallington and Wiesen (2014). As with the current work, the estimate of N_2O emissions from LDVs by Wallington and Wiesen (2014) includes cold-start emissions. While further investigations are needed to better clarify vehicle N_2O emissions, it is clear that absolute N_2O emissions from road vehicles are approximately 4 orders of magnitude lower than CO_2 emissions (see Figure S3).

Popa et al. (2014) reported the results of measurements of vehicle exhaust in the Islisberg tunnel in Switzerland in 2011. The traffic through the tunnel was 85% personal vehicles and 5% heavy goods vehicles with the remaining 10% non-specified but presumably vans, motorcycles, buses, etc. Popa et al. reported volume ratios of: CO/CO_2, $(4.15\pm0.34) \times 10^{-3}$; N_2O/CO_2, $(1.8\pm0.2) \times 10^{-5}$; and CH_4/CO_2, $(4.6\pm0.2) \times 10^{-5}$ which correspond to emission ratios of $(2.64\pm0.22) \times 10^{-3}$ g CO $(g\ CO_2)^{-1}$, $(1.8\pm0.2) \times 10^{-5}$ g N_2O $(g\ CO_2)^{-1}$, and $(1.7\pm0.1) \times 10^{-5}$ g CH_4 $(g\ CO_2)^{-1}$. The values obtained assuming an LDV:HDV ratio in the tunnel of 85:5 from the g $(g\ CO_2)^{-1}$ emission data in Figure S3 from the present work are 0.018 g CO $(g\ CO_2)^{-1}$, 5.6×10^{-5} g N_2O $(g\ CO_2)^{-1}$, and 1.7×10^{-4} g CH_4 $(g\ CO_2)^{-1}$. The emission rates measured in the tunnel for CO, N_2O, and CH_4 are factors of 6, 3, and 10 lower than estimated for the on-road fleet in Europe in the present work. The difference presumably reflects the fact that all vehicles in the tunnel have warmed engines and catalytic exhaust treatment systems.

In summary, where comparison is possible our estimates of the magnitude and trends of non-CO_2 emissions of the global LDV and HDV fleets are generally consistent, within a factor of 2, with field measurements and with existing databases.

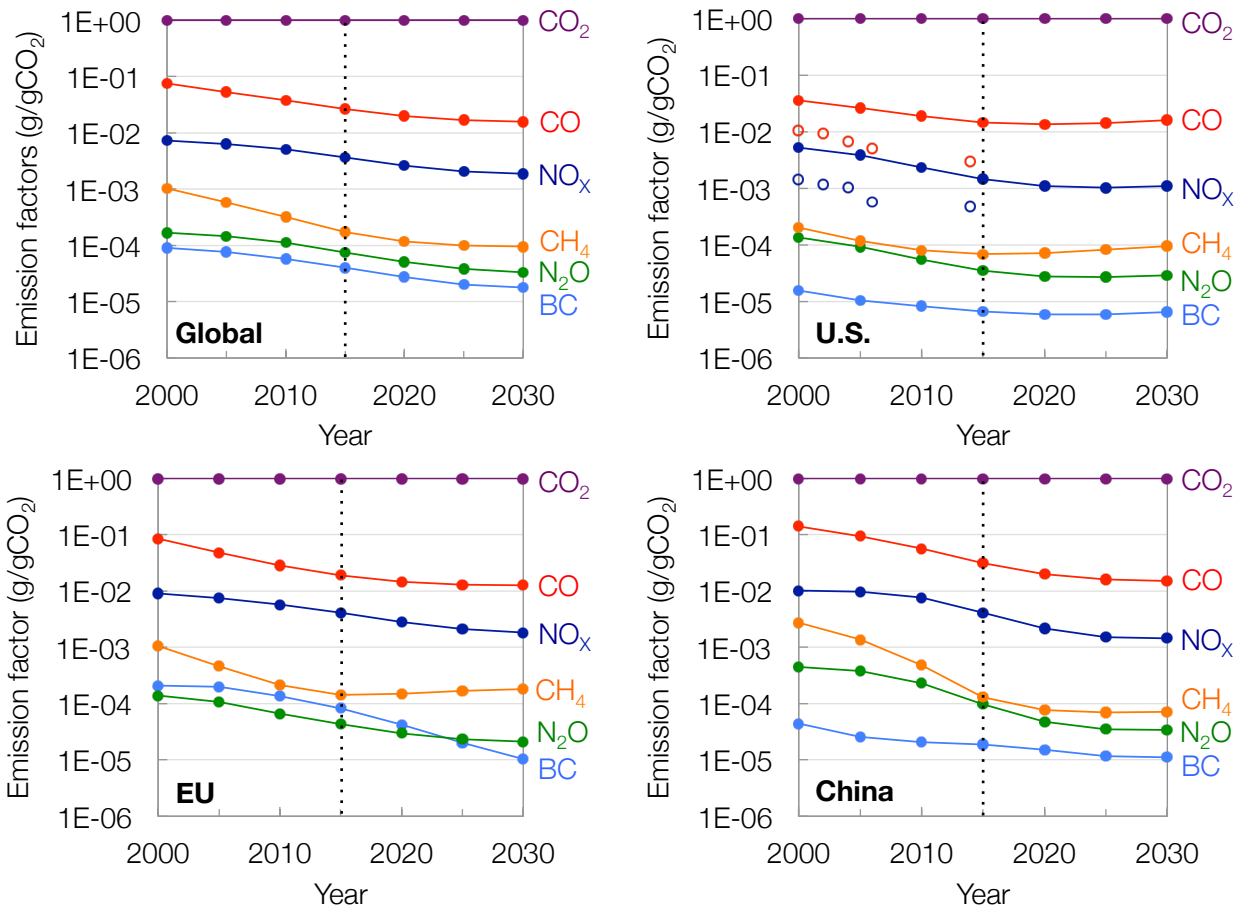

Figure S1: Light-duty tank-to-wheel emission factors of CO_2 (purple), CO (red), NO_x (dark blue), CH_4 (orange), N_2O (green), and black carbon (BC, light blue) emissions from the global, U.S., EU, and China fleets, expressed in g per g CO_2. The data indicated by open circles in the U.S. plot are measurements of CO (red) and NO_x (blue) emissions by Bishop and Stedman (2015).

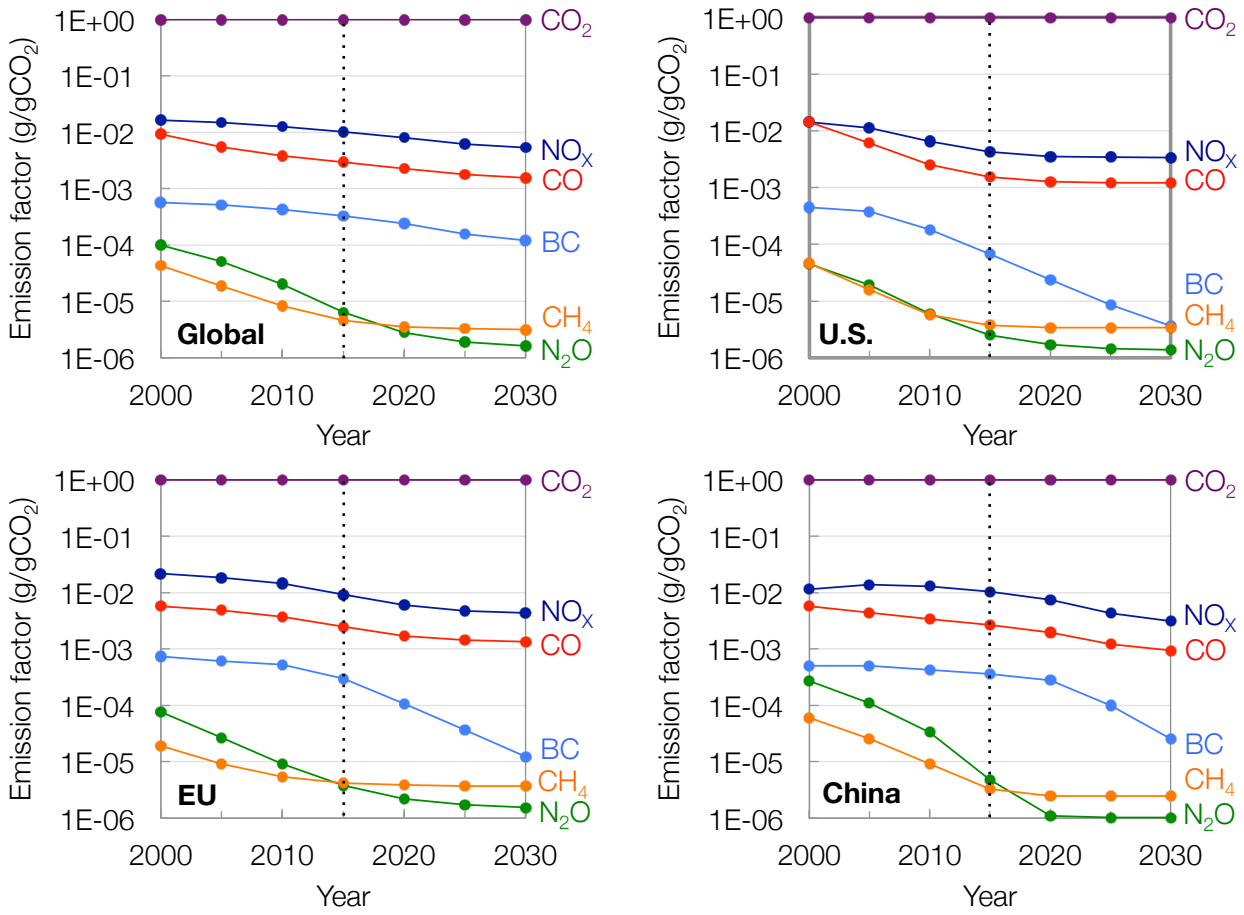

Figure S2: Heavy-duty tank-to-wheel emission factors of CO_2 (purple), CO (red), NO_x (dark blue), CH_4 (orange), N_2O (green), and black carbon (BC, light blue) emissions from the global, U.S., EU, and China fleets, expressed in g per g CO_2.

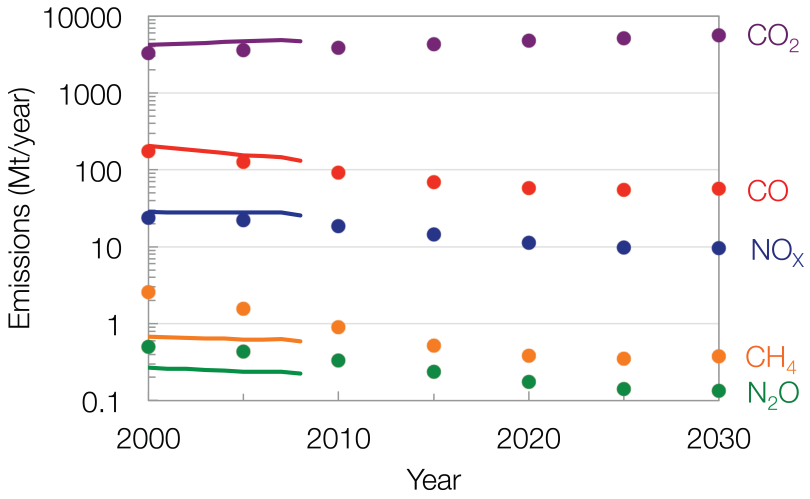

Figure S3: Global tank-to-wheel (tailpipe) emissions of CO_2 (purple), CO (red), NO_x (dark blue), CH_4 (orange), and N_2O (green) emissions, expressed in Mt. The dot symbols spaced every 5 years are for the combined LDV and HDV fleet estimated in the present work. Annual data from 2000 to 2008 connected by lines are from the EDGAR database for on-road transportation.

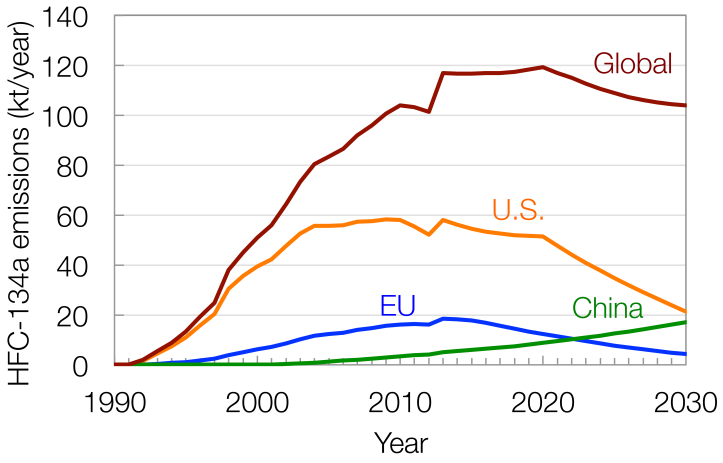

Figure S4: Vehicle emissions of HFC-134a: global (brown), U.S. (orange), EU (blue), and China (green) from Velders et al. (2015).

S4. Well-to-wheel emission intensity trends

This paper presents historical and projected future trends in TTW emission intensities of LDVs and HDVs (Figures 1 and 2). We choose this system boundary to highlight the impact of tailpipe emission standards, the main driver of the substantial reductions in non-CO_2 emissions intensities over the past decade. Emission intensities of CO_2 and many non-CO_2 climate pollutants are dominated by the vehicle

use phase, meaning that changes in TTW and well-to-wheel (WTW) emission intensities are similar (with WTW intensities being higher in absolute terms due to the larger system boundary). However, in the case of CH_4, upstream emissions from fuel production are a dominant share of total emissions, and TTW and WTW intensities differ. For example, CH_4 intensities of HDVs are much flatter when viewed from a WTW, rather than TTW, perspective. These results underscore the importance of considering broader system boundaries that take into account the non-combustion impacts of vehicle use. Figures S5 and S6 show WTW emission intensity trends for LDVs and HDVs, respectively, corresponding to the TTW emission plots in Figures 1 and 2 in the main paper.

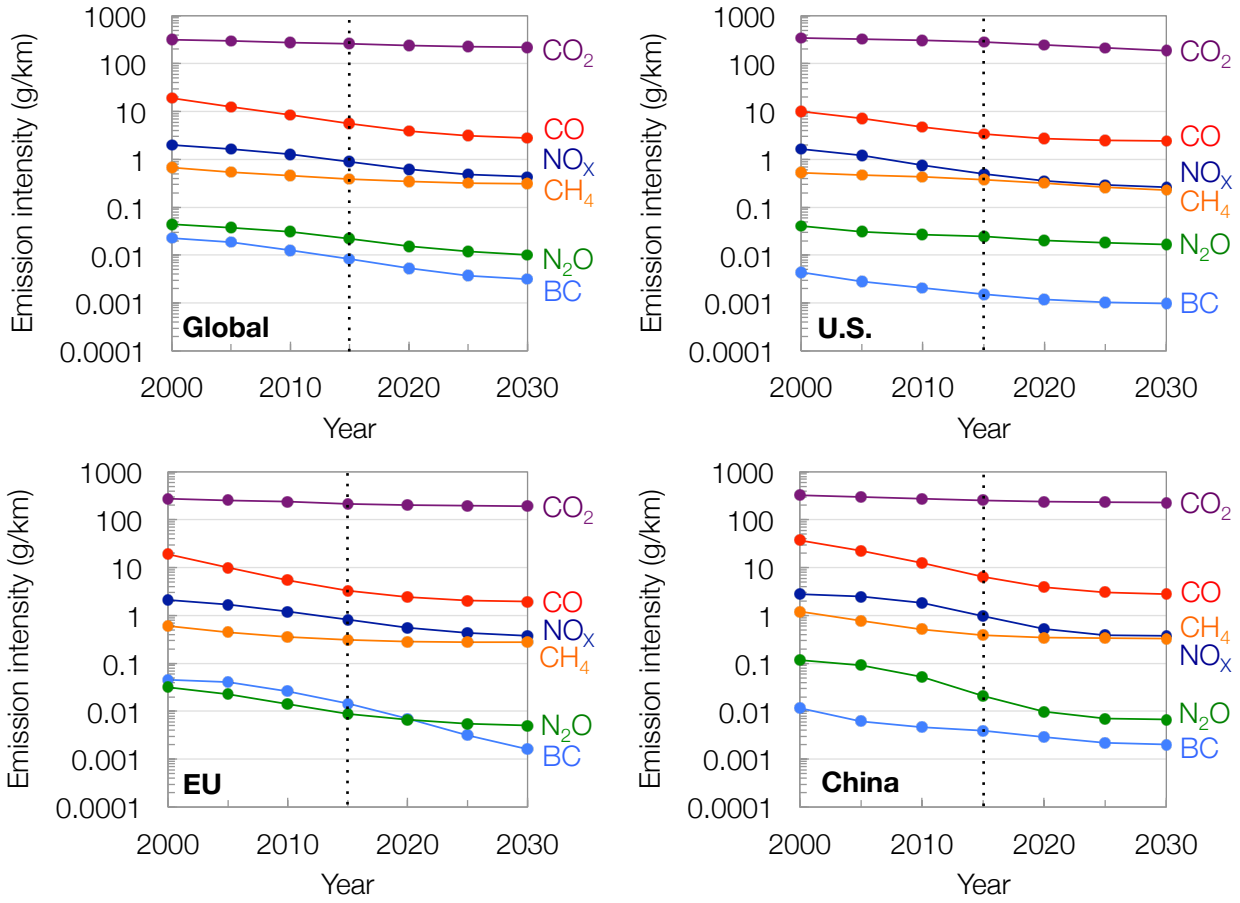

Figure S5: Light-duty vehicle well-to-wheel CO_2 (purple), NO_x (dark blue), CO (red), black carbon (BC, light blue), CH_4 (orange) and N_2O (green) emission intensities from the global, U.S., EU and China fleets.

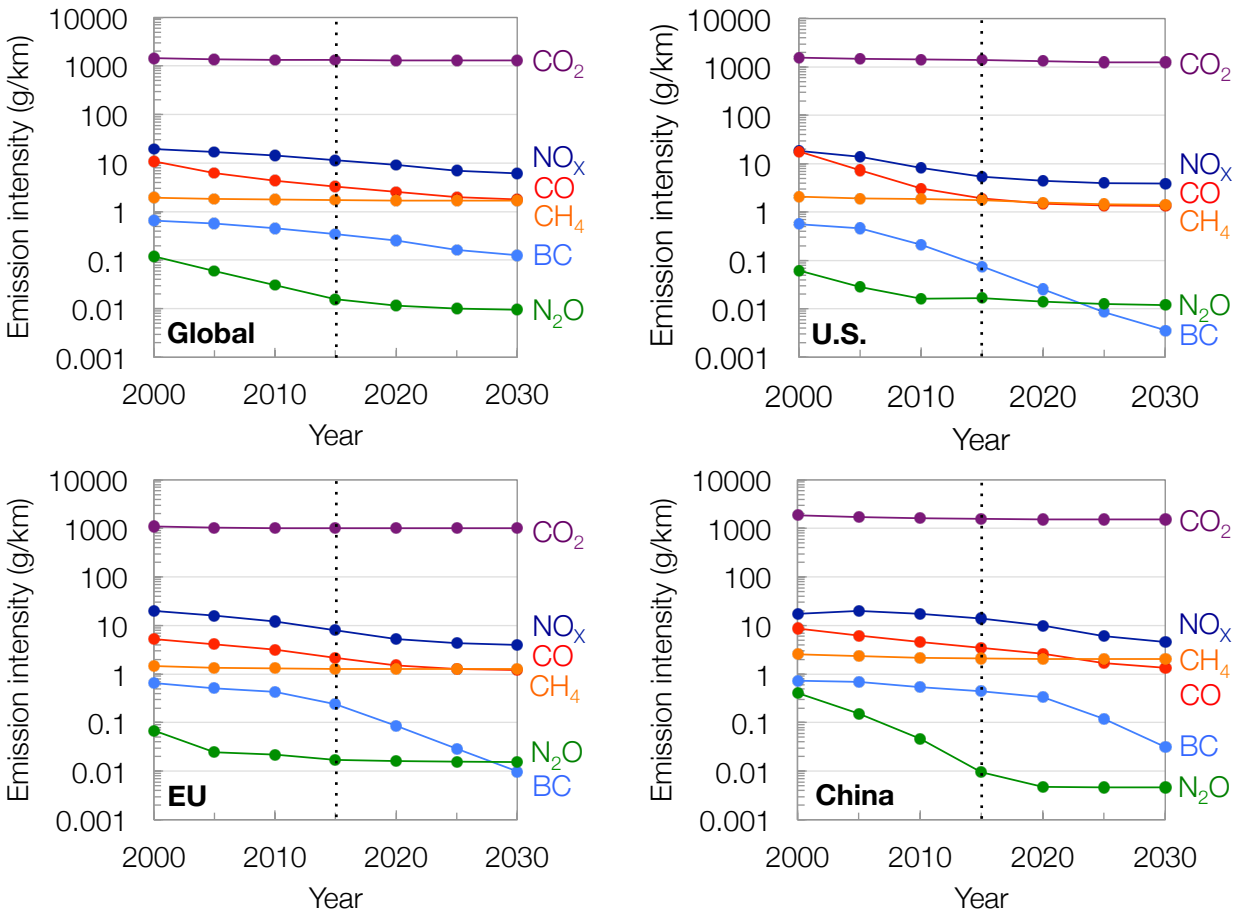

Figure S6: Heavy-duty vehicle well-to-wheel CO_2 (purple), NO_x (dark blue), CO (red), black carbon (BC, light blue), CH_4 (orange) and N_2O (green) emission intensities from the global, U.S., EU and China fleets.

S5. Emissions from vehicle manufacturing

Figure S7 below shows vehicle emissions, including both the fuel and the vehicle cycle, compared against intensity targets derived from U.S. climate policy goals. Emission estimates are taken from GREET and, in addition to WTW emissions, include emissions from vehicle manufacturing, maintenance (including tire replacement), recycling, and disposal. Emissions from battery manufacturing can be significant for electric vehicles (EVs) because this process is energy intensive (Hawkins et al 2013, Kim et al 2016). We use GREET's vehicle cycle emission estimates in the plots below, which for EVs is at the lower end of vehicle cycle emissions estimates.

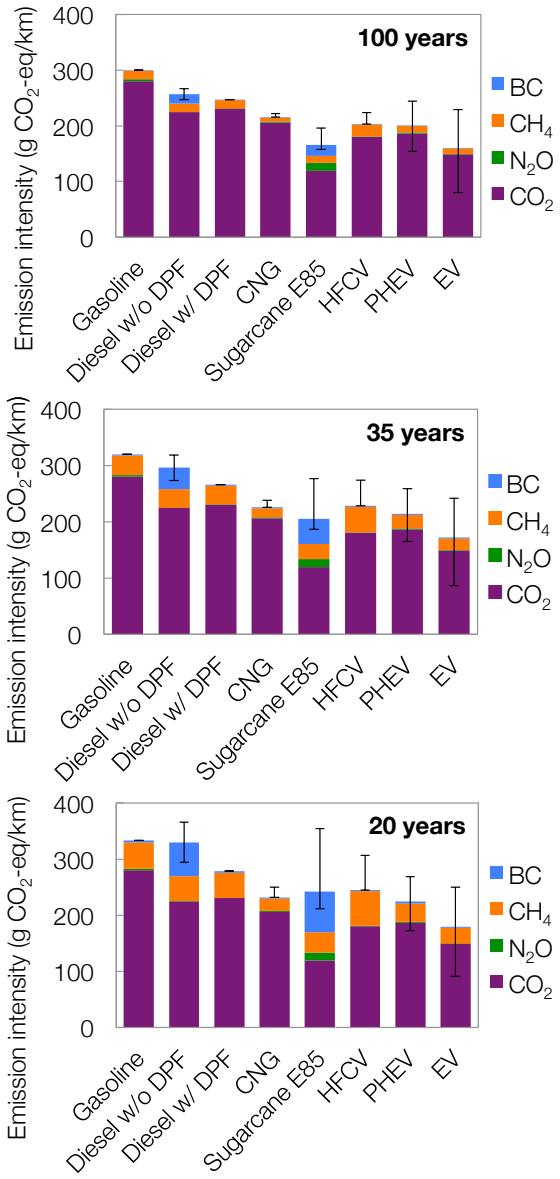

Figure S7: Life cycle emission intensities, including well-to-wheel fuel cycle emissions and vehicle cycle emissions, of eight vehicle/fuel pairs using time horizons of 100 years (top panel), 35 years (middle panel), and 20 years (bottom panel) to compare the integrated climate impact of different forcing agents to that of CO_2. Error bars capture ranges in black carbon (BC) emissions of diesel vehicles without filters, CH_4 leakage and venting in the natural gas supply chain for compressed natural gas (CNG) and hydrogen fuel cell vehicles (HFCVs), and greenhouse gas emission intensity of the electric grid for electric vehicles (EVs) and plug-in hybrid electric vehicles (PHEVs). The low end for the electricity mix corresponds to Brazil's mix, as an example of a low-carbon mix, and the high end corresponds to China's mix.

S6. Greenhouse gas equivalency metrics

Figure S8 shows the cumulative radiative forcing due to a pulse emission of CH_4 or BC, relative to CO_2, as a function of the time horizon. The impact value placed on these short-lived climate pollutants (SLCPs)

increases as the time horizon shrinks. Even after an impact measure (e.g., cumulative radiative forcing) and time horizon are chosen, there are additional uncertainties in the equivalency value assigned to SLCPs relative to CO_2. These include uncertainties in the direct radiative efficiencies and lifetimes of the climate forcing agents as well as the treatment of various indirect effects. We use parameter estimates from the Intergovernmental Panel on Climate Change in our metric calculations (IPCC 2013). The resulting metric values are given in Table S3. The lifetimes and radiative efficiencies for BC (as well as CH_4 and N_2O) used by the IPCC are also provided in Shine *et al.* (2015). These estimates include the indirect effects of CH_4 emissions on ozone and stratospheric water vapor, of N_2O emissions on CH_4 thorough various processes, and of BC on aerosol radiation interaction and snow and ice albedo.

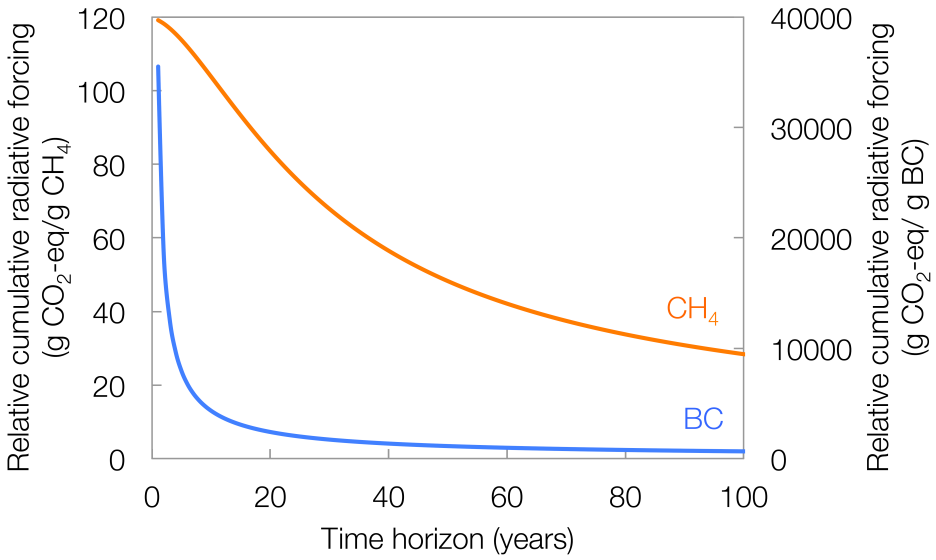

Figure S8: Cumulative radiative forcing of CH_4 (orange) and black carbon (BC, light blue), relative to CO_2, over a range of time horizons. Equivalency values may be assigned to greenhouse gases based on their cumulative radiative forcing over a fixed time horizon, as with the global warming potential (GWP), or a time horizon that depends on when a climate policy target is expected to be reached. The relative emphasis placed on short-lived climate pollutants (SLCPs, e.g. CH_4 and BC) increases as the time horizon decreases.

Table S3: Metric values in g CO_2-equivalent per g CH_4, N_2O, or black carbon (BC) for 20-year, 35-year, and 100-year time horizons.

Time horizon	CH_4	N_2O	BC
20-year	84	265	2410
35-year	62	265	1515
100-year	28	265	655

Metric values for BC and other very-short-lived, not-well-mixed forcing contributions are particularly uncertain, given the number of processes involved and the fact that the impacts depend on the location and time of year. The lifetimes and radiative efficiencies we use in calculating equivalency metrics for BC are meant to represent a global average. While these values capture some but not all indirect effects, they also fall within the large range of uncertainties for metrics that capture these effects more fully. Bond *et al.* (2013) report an uncertainty range for the GWP(100) for BC of 140-1100 when considering only direct effects and 100-1700 when considering a full set of indirect effects (in units of g CO_2-equivalent per g BC). The uncertainty ranges for the GWP(20) are 420-3700 and 270-6200 when considering direct only and indirect effects, respectively (again in units of g CO_2-equivalent per g BC). These uncertainties highlight the need for further research to understand the climate impacts of BC to inform the evaluation of BC-heavy vehicles technologies and other emissions sources.

Vehicle use results in a number of other emissions of near-term forcing agents that contribute directly and indirectly to climate change. The magnitude and even direction of these radiative forcing contributions is highly uncertain. Examples include organic carbon (OC), NO_x, and CO. OC is co-emitted with BC in differing proportions depending on the emissions source and has a net cooling effect. Emissions from diesel (without a particulate filter) are overwhelmingly BC. Emissions in the sugar cane E85 fuel cycle have a slightly higher OC:BC ratio, but the net forcing effect of the combined OC and BC emissions is still strongly positive (Cai *et al.* 2014).

NO_x does not have a direct contribution to radiative forcing of climate, but it has indirect impacts by virtue of its participation in chemistry leading to the formation of tropospheric ozone and organic nitrate aerosol (IPCC 2013). Increased formation of tropospheric ozone leads to increased OH radical flux and decreased CH_4 atmospheric lifetime (a third indirect effect). Assessing the combined effect of the three competing indirect contributions to radiative forcing is complex. GWP estimates for NO_x vary widely and lie in the range -159 to -11 on a 100-year horizon (g CO_2-eq (g NO_x)$^{-1}$, IPCC 2013). While we note that it is likely that NO_x emissions offset to a small degree the radiative forcing from other vehicle emissions in the present study, we confine our interest to vehicle emissions with direct impacts on radiative forcing (CO_2, BC, CH_4, HFCs, and N_2O).

CO also does not have a direct contribution to radiative forcing of climate, but it has an indirect effect on radiative forcing through effects on O_3 and CH_4. The IPCC estimates a GWP(100) for CO of 1.9 g CO_2-eq (g CO)$^{-1}$. While these values are uncertain, they suggest that the climate impacts of vehicle CO and

NO_x emissions are likely low relative to the contributions we examine (e.g., CO_2, CH_4, N_2O, BC) in our technology comparisons (IPCC 2013).

References

G. A. Bishop and D. H. Stedman, On-road remote sensing of automobile emissions in the Chicago area: Fall 2014, CRC Report E-106, 2015, http://www.crcao.org/reports.

T. C. Bond, S. J. Doherty, D. W. Fahey, P. M. Forster, T. Berntsen, B. J. DeAngelo, et al., Bounding the role of black carbon in the climate system: A scientific assessment, *J. Geophys. Res. Atmos*., 2013, 118, 5380-5552.

H. Cai, A. Burnham, and M. Wang, Updated emission factors of air pollutants from vehicle operations in GREET using MOVES, Argonne National Laboratory, 2013.

D. C. Carslaw, S. D. Beevers, J. E. Tate, E. Westmoreland, and M. L. Williams, Recent evidence concerning higher NO_x emissions from passenger cars and light duty vehicles, *Atmos. Environ.*, 2011, 45, 7053–7063.

D. C. Carslaw, T. P. Murrells, and J. Andersson, Have vehicle emissions of primary NO_2 peaked?, *Farad. Discuss.*, 2016 189, 439-454.

D. C. Carslaw and G. Rhys-Tyler, New insights from comprehensive on-road measurements of NO_x, NO_2 and NH_3 from vehicle emission remote sensing in London, UK, *Atmos. Environ.*, 2013, 81, 339-347.

Y. Chen and J. Borken-Kleefeld, Real-driving emissions from cars and light commercial vehicles: Results from 13 years remote sensing at Zurich/CH, *Atmos. Environ.*, 2014, 88, 157–164.

Y. Deng, C. Chen, Q. Li, Q. Hu, H. Yuan, J. Li, Y. Li, Measurements of real-world vehicle CO and NO_x fleet average emissions in urban tunnels of two cities in China, *Atmos. Environ.*, 2015, 122, 417-426.

A. Elgowainy, J. Han, J. Ward, F.Joseck, D. Gohlke, A. Lindauer, T. Ramsden, M. Biddy, M. Alexander, S. Barnhart, I. Sutherland, L. Verduzco, T.J. Wallington, Cradle-to-Grave Lifecycle Analysis of U.S. Light Duty Vehicle-Fuel Pathways: A Greenhouse Gas Emissions and Economic Assessment of Current (2015) and Future (2025–2030) Technologies, Argonne National Laboratory Report ANL ESD -16/7, 2016.

European Commission, Joint Research Centre (JRC)/Netherlands Environmental Assessment Agency (PBL). Emission Database for Global Atmospheric Research (EDGAR), release EDGARv4.2 FT2012, http://edgar.jrc.ec.europa.eu, 2014.

C. E. Fegraus, C. J. Domke, J. Marzen, Contribution of the vehicle population to atmospheric pollution, Society of Automotive Engineers Technical Paper, 1973, 730530.

GREET 2016, Argonne National Laboratory, https://greet.es.anl.gov/index.php?content=greetdotnet, Accessed January 27, 2017.

T. R. Hawkins, B. Singh, G. Majeau-Buttez, and A. H. Stromman, Comparative environmental life cycle assessment of conventional and electric vehicles, *J. Indust. Ecol.*, 2013, 17, 53-64.

International Council on Clean Transportation (ICCT) Roadmap Model, 2012, http://www.theicct.org/global-transportation-roadmap-model, downloaded December 2016.

IPCC, 2013, Climate Change 2013: The Physical Science Basis. Contribution of Working Group I to the Fifth Assessment Report of the Intergovernmental Panel on Climate Change [Stocker, T. F., D. Qin, G. K. Plattner, M. Tignor, S. K. Allen, J. Boschung, A. Nauels, Y. Xia, V. Bex and P. M. Midgley (eds.)]. Cambridge University Press, Cambridge, United Kingdom and New York, NY, USA, 1535 pp.

H. C. Kim, T. J. Wallington, R. Arsenault, C. Bae, S. Ahn, and J. Lee, Cradle-to-gate emissions from a commercial electric vehicle Li-ion battery: A comparative analysis, *Environ.Sci. Technol.*, 2016, 50, 7715-7722.

M. Miotti, G. J. Supran, E. J. Kim, and J. E. Trancik. Personal vehicles evaluated against climate change mitigation targets. *Environ. Sci. Technol.*, 2016, **50**, 10795-10804.

E. K. Nam, T. E. Jensen, T. J. Wallington, Methane emissions from vehicles, *Environ. Sci. Technol.*, 2004, **38**, 2005-2010.

M. E. Popa, M. K. Vollmer, A. Jordan, W. A. Brand, S. L. Pathirana, M. Rothe, and T. Röckmann, Vehicle emissions of greenhouse gases and related tracers from a tunnel study: $CO:CO_2$, $N_2O:CO_2$, $CH_4:CO_2$, $O_2:CO_2$ ratios, and the stable isotopes ^{13}C and ^{18}O in CO_2 and CO, *Atmos. Chem. Phys.*, 2014, 14, 2105-2123.

K. P. Shine, R. P. Allan, W. J. Collins, J. S. Fuglestvedt, Metrics for linking emissions of gases and aerosols to global precipitation changes, *Earth Syst. Dynam.*, 2015, **6**, 525-540.

J. L. Sullivan, R. E. Baker, B. A. Boyer, R. H. Hammerle, T. E. Kenney, L. Muniz, T. J. Wallington, CO_2 emission benefit of diesel (versus gasoline) powered vehicles, *Environ. Sci. Technol.*, 2004, 38, 3217-3223.

N. Toenges-Schuller, C. Schneider, A. Niederau, R. Vogt, S. Hausberger, Modelling the effect on air quality of Euro 6 emission factor scenarios, *J. Earth Sci. Geotech. Eng.*, 2016, **6**, 227-244.

G. J. M. Velders, G. P. Geilenkirchen and R. de Lange, Higher than expected NO_x emission from trucks may affect attainability of NO_2 limit values in the Netherlands, *Atmos. Environ.*, 2011, **45**, 3025–3033.

G. J. M. Velders, D. W. Fahey, J. S. Daniel, S. O. Andersen, M. McFarland, Future atmospheric abundances and climate forcings from scenarios of global and regional hydrofluorocarbon (HFC) emissions, *Atmos. Environ.*, 2015, **123**, 200-209.

T. J. Wallington, E. W. Kaiser, J. T. Farrell, Automotive fuels and internal combustion engines: A chemical perspective, *Chem. Soc. Rev.*, 2006, **35**, 335-347.

T. J. Wallington, J. L. Sullivan, and M. D. Hurley, Emissions of CO_2, CO, NO_x, HC, PM, HFC-134a, N_2O and CH_4 from the global light duty vehicle fleet, *Meteorol. Z.*, 2008, 17, 109-116.

T. J. Wallington and P. Wiesen, N_2O emissions from global transportation, *Atmos. Environ.*, 2014, 94, 258-262.

J. M. Wang, C.-H. Jeong, N. Zimmerman, R. M. Healy, D. K. Wang, F. Ke, and G. J. Evans, Plume-based analysis of vehicle fleet air pollutant emissions and the contribution from high emitters, *Atmos. Meas. Tech.*, 2015, **8**, 3263–3275.

M. Weiss, P. Bonnel, R. Hummel, A. Provenza and U. Manfredi, On-road emissions of light-duty vehicles in Europe, *Environ. Sci. Technol.*, 2011, 45, 8575–8581.

M. Weilenmann, J.-Y. Favez, R. Alvarez, Cold-start emissions of modern passenger cars at different low ambient temperatures and their evolution over vehicle legislation categories, *Atmos. Environ.*, 2014, 43, 2419-2429.

D. Westerdahl, X. Wang, X. Pan, and K. M. Zhang, Characterization of on-road vehicle emission factors and microenvironmental air quality in Beijing, China., *Atmos. Environ.*, 2009, 43, 697-705

World Business Council for Sustainable Development, Mobility 2030: Meeting the challenges to sustainability. The Sustainable Mobility Project, Full Report 2004. http://www.wbcsd.org/Projects/smp2/Resources/Mobility-2030-Meeting-the-challenges-to-sustainability-Full-Report-2004

Y. B. Zeldovich, The oxidation of nitrogen in combustion and explosions, *Acta Phys.-Chim. Sin.*, 1946, 21, 577–628.

Y. Zhou, L. Fu, and L. Cheng, Characterization of In-Use Light-Duty Gasoline Vehicle Emissions by remote sensing in Beijing: Impact of recent control measures, *J. Air & Waste Manage. Assoc.*, 2007, 57, 1071–1077.